

Closed-Form Expressions for the Numerical Dispersion and Reflection in FEM Simulations Involving Biaxial Materials

Arnan Mitchell, David M. Kokotoff, *Member, IEEE*, and Michael W. Austin, *Member, IEEE*

Abstract—Closed-form expressions for the numerical errors caused by finite-element discretization of problems involving materials of biaxial permittivity and permeability tensors are developed. In particular, we derive expressions for the numerical dispersion and reflection in both first-order node and edge basis function finite-element formulations in an equilateral triangular mesh. Results using these closed-form expressions are compared to practical numerical simulations. The application of these expressions to the analysis of the performance of the perfectly matched layer boundary is suggested.

Index Terms—Finite-element methods, numerical errors, perfectly matched layer (PML).

I. INTRODUCTION

THE Finite-element method (FEM) has become an essential tool for research in the field of electromagnetic and integrated optic device design. As available numerical processing power improves, more sophisticated devices, in particular integrated optic devices, can be simulated. It is important to understand the numerical errors imposed by the approximations made in the FEM model so that an efficient and accurate simulation can be conducted. Thus, it is necessary to quantify the numerical errors resulting from the finite-element discretization.

Numerical dispersion resulting from finite-element discretization has been investigated in great detail for many formulations of the finite-element method in isotropic media [1]–[3]. Many interesting problems in the area of integrated optics involve the material lithium niobate (LiNbO_3) since it exhibits a strong electrooptic coefficient and low optical propagation loss. LiNbO_3 also exhibits a uniaxial permittivity tensor, and hence models for simulating devices based on this material must account for the possibility of anisotropic material tensors. Hence in this investigation, the numerical dispersion resulting from finite-element discretization of problems involving biaxial materials is derived.

Another aspect of simulation where the consideration of numerical errors introduced by the FEM become important is the imposition of boundary conditions. Recently, a highly efficient boundary condition called the perfectly matched layer (PML)

has been developed [4]. The PML is an absorbing material that can be engineered to perfectly match a neighboring material, and hence produce precisely zero reflection at all frequencies and angles of incidence. Investigations of the implementation of PML boundary conditions in FEM simulations have reported reflections from the interface between the PML layer and the material to which it is matched [5]. These reflections have been attributed to discretization error in the FEM. Since the tensor form of the PML material is uniaxial, a quantitative understanding of the numerical reflection from interfaces between anisotropic materials in the FEM method is also necessary to efficiently implement such PML boundaries.

An investigation [6] has reported closed-form expressions for the reflection coefficient from a PML interface in a finite-difference time-domain (FDTD) model on a rectangular grid for interfaces between isotropic media and a PML truncation. Similarly, in this investigation, numerical dispersion and reflection that results from the finite-element discretization using first-order triangular edge and node elements are investigated. Further, the derivation is conducted assuming a general class of problem involving media of biaxial material tensor, of which a material/PML interface can be considered a special case. This investigation is thus applicable to the analysis of the performance of the generalized biaxial PML [7].

This paper derives a closed-form expression for the numerical dispersion and numerical reflection resulting from an equilateral triangular finite-element discretization of a general two-dimensional geometry involving biaxial media. The derivation is performed for both first-order node and first-order edge basis functions. The final expressions are compared to the numerical dispersion and reflection observed in a practical simulation of discontinuities in a dielectric-loaded parallel plate waveguide. This comparison verifies the applicability of the assumption of a perfect hexagonal mesh to practical meshes involving a distribution of imperfect triangles at various orientations.

II. THEORY

Solutions obtained using numerical methods are never exact. In the limit of infinite unknowns, due to either infinite discretization or basis function order, the numerical solution should approach the exact solution. For obvious reasons, it is not possible to solve a problem with infinite unknowns, and often it is not practical to solve problems with even large numbers of unknowns. In most cases, it is desirable to solve a problem with the minimum requirements to achieve a nominal tolerable

Manuscript received October 27, 1999; revised April 28, 2000.

A. Mitchell and M. W. Austin are with the Department of Communication and Electronic Engineering, Royal Melbourne Institute of Technology, Melbourne VIC 3001 Australia.

D. M. Kokotoff was with the Royal Melbourne Institute of Technology, Melbourne VIC 3001 Australia. He is now with Gabriel Electronics, Scarborough, ME 04074 USA.

Publisher Item Identifier S 0018-926X(01)02294-3.

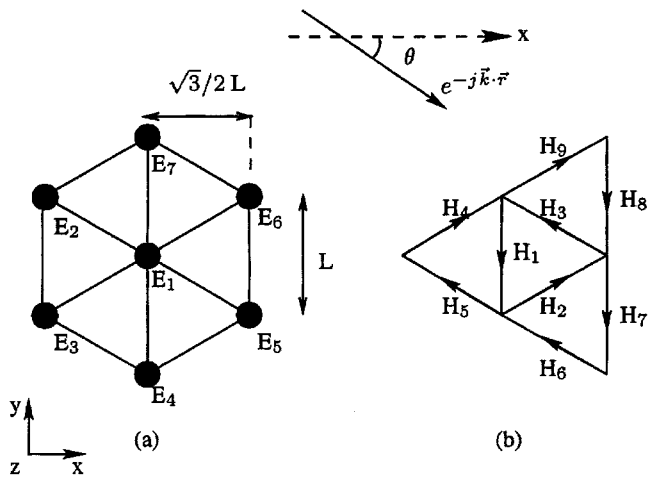


Fig. 1. The unit cell for (a) node and (b) edge basis functions.

error. This paper considers errors due to finite discretization of first-order basis functions in biaxial media, leaving the investigation of the errors associated with higher order elements for future work.

The errors due to finite discretization can be divided into two categories: 1) the numerical dispersion (and also dissipation) that occurs as a simulated wave propagates across uniform elements of the same medium and 2) numerical reflection errors that occur as the simulated wave crosses a boundary between two different media. Expressions for these two types of errors for a finite-element simulation using first-order edge and node basis functions are developed in the following two sections.

A. Numerical Dispersion Errors

The numerical dispersion error is the difference between the dispersion of a simulated wave propagating through a uniform medium, as modeled using a discretized finite method, and the dispersion of the true solution. If the dispersion is considered as a complex quantity, it encompasses numerical dissipation in the same uniform medium. Warren and Scott [1]–[3] have derived the numerical dispersion for a number of mesh types including triangular, rectangular, and quadrilateral for both edge and node basis functions and for various interpolation orders. These, however, have been calculated assuming isotropic media. This section derives expressions for the numerical dispersion for first-order two-dimensional equilateral triangular node and edge finite-element basis functions in arbitrary biaxial media. The procedure follows that of [1] and [2], but the treatment is extended to include biaxial material tensors.

Consider the meshes depicted in Fig. 1. The two-dimensional space is discretized uniformly using equilateral triangular node and edge basis functions, respectively. As depicted in Fig. 1, each of the edge and node unit cells comprises a superposition of the basis functions that span all of the two-dimensional space. A plane wave is projected onto this mesh, forcing equivalent basis functions in each unit cell to differ by only a phase shift. Using the finite-element local matrix to relate the subcomponents of each unit cell and the relative phase shift between unit cells, a set of coupled equations can be derived, the solution to which yields the numerical propagation constant.

Performing this procedure on the unit cell depicted in Fig. 1(a), assuming biaxial material tensors of the form

$$\bar{\bar{\epsilon}}_r = \begin{bmatrix} \epsilon_x & 0 & 0 \\ 0 & \epsilon_y & 0 \\ 0 & 0 & \epsilon_z \end{bmatrix} \quad \bar{\bar{\mu}}_r = \begin{bmatrix} \mu_x & 0 & 0 \\ 0 & \mu_y & 0 \\ 0 & 0 & \mu_z \end{bmatrix} \quad (1)$$

results in the transcendental equation

$$(A + 2C) + D \cos(2b) + 2B \cos(a) \cos(b) = 0 \quad (2)$$

for node basis functions [8, p. 80], where

$$A = 1 - \frac{8}{c_y^2} \quad (3)$$

$$B = 1 + \frac{8}{c_y^2} \quad (4)$$

$$C = 1 - \frac{6}{c_x^2} - \frac{2}{c_y^2} \quad (5)$$

$$D = 1 + \frac{12}{c_x^2} - \frac{4}{c_y^2} \quad (6)$$

$$a = \sqrt{3}/2 c_y \beta \cos(\theta) \quad (7)$$

$$b = 1/2 c_x \beta \sin(\theta) \quad (8)$$

$$c_x = k_0 \sqrt{\epsilon_z \mu_x} L \quad (9)$$

$$c_y = k_0 \sqrt{\epsilon_z \mu_y} L \quad (10)$$

for a TE to z polarized plane wave, or

$$c_x = k_0 \sqrt{\mu_z \epsilon_x} L \quad (11)$$

$$c_y = k_0 \sqrt{\mu_z \epsilon_y} L \quad (12)$$

for a TM to z polarized plane wave, propagating at an angle θ to the x -axis. L is the edge length of the equilateral triangle, and β is the numerical dispersion, which should ideally be one.

A similar treatment can be applied to a hexagonal mesh of equilateral, triangular edge basis functions, as described in [8, pp. 234–236] and depicted in Fig. 1(b). Applying a plane wave phase relation and finite-element local matrix to relate the basis functions that span the space allows the numerical dispersion to be computed as the solution of

$$\begin{aligned} & D' (A'D' - B'^2) \cos^2(b) \\ & = C' (A'C' - B'^2) - (C' - D') B'^2 \cos(a) \cos(b) \end{aligned} \quad (13)$$

where

$$A' = -c_x^2 - 9c_y^2 + 96 \quad (14)$$

$$B' = -c_x^2 + 3c_y^2 + 96 \quad (15)$$

$$C' = -7c_x^2 - 3c_y^2 + 96 \quad (16)$$

$$D' = 5c_x^2 - 3c_y^2 + 96. \quad (17)$$

If isotropic media are used, (2) and (13) reduce to the isotropic relations described in [2] and [3] as expected.

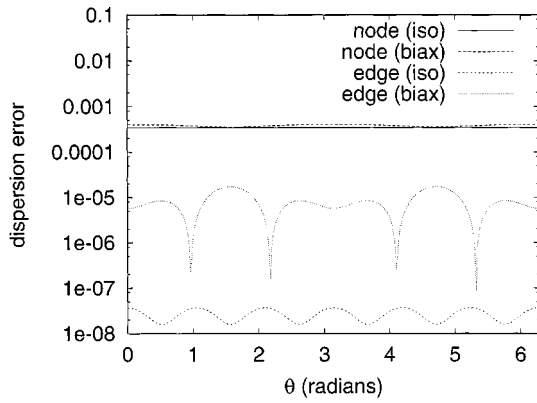


Fig. 2. Comparison of the numerical dispersion predicted for node and edge basis functions, given by (2) and (13), respectively, in both isotropic and biaxial media as a function of propagation angle θ . For each case, $c_x = 0.1$, with $c_y = 0.1$ for the isotropic case and $c_y = 0.11$ for the biaxial case.

Fig. 2 presents the predicted dispersion error, defined as $(1 - \beta)$, as a function of propagation angle for both node and edge basis functions for both isotropic and anisotropic media. Comparing the plots for node and edge basis functions for isotropic media, it is evident that the level of predicted dispersion error for edge basis functions is far lower than for nodes. Further, as discussed in [2], the numerical dispersion error of the edge basis functions exhibit far more inherent anisotropy due to the mesh orientation.

Comparing the dispersion error of node and edge basis functions in biaxial media in Fig. 2, the anisotropy has only slightly increased the numerical dispersion along the major axis for the nodes but has significantly altered the dispersion error for the edge basis functions, raising the level of error exhibited by the edge functions for all but a few specific orientations. It is worth noting that the dispersion error for these edge elements is still two orders of magnitude smaller than the equivalent nodal case. Thus, for a mesh of randomly oriented triangular edge basis functions of first order, even mild anisotropy should cause a significant increase in overall dispersion error. A similar increase in dispersion error observed for nonequilateral triangular edge elements has been observed in [3].

B. Numerical Reflection

When modeling an interface between two different materials using a finite method, numerical errors will again result due to the finite discretization. First, dispersion errors, as described in the previous section, will slightly alter the propagation characteristics of the waves on either side of the boundary causing small errors in the resulting reflection. Further, errors caused by the finite method's imperfectly imposing boundary conditions across the interface of the two elements will also contribute to reflection error. This section develops a closed-form expression that may be used to calculate the reflectance error due to both of these factors.

A similar approach to that used in Section II-A is employed to calculate this reflection error in closed form. Consider the situation depicted in Fig. 3(a). Here, a cell straddling the interface

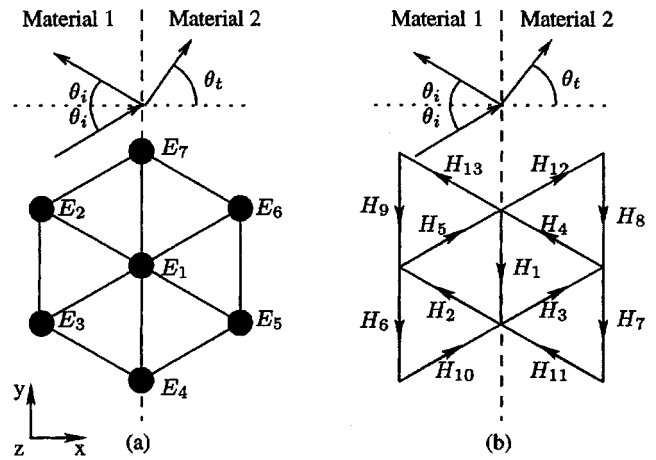


Fig. 3. A portion of the hexagonal mesh straddling an interface between Material 1 and 2 with (a) nodal and (b) edge unknowns labeled. The plane wave angle of incidence and transmission, θ_i and θ_t , respectively, are also indicated.

between two materials is defined. The elements composing this unit cell are chosen such that they span all space on either side of the boundary. Again, a plane wave is projected onto this mesh. Relating translated elements by a phase shift, the field values at each node can be written

$$\begin{aligned} E_1 &= (1 + r) & E_2 &= e^{-ja_1} e^{jb_1} + r e^{ja_1} e^{jb_1} \\ E_3 &= e^{-ja_1} e^{-jb_1} + r e^{ja_1} e^{-jb_1} & E_4 &= (1 + r) e^{-2jb_1} \\ E_5 &= (1 + r) e^{ja_2} e^{-jb_2} & E_6 &= (1 + r) e^{ja_2} e^{jb_2} \\ E_7 &= (1 + r) e^{2jb_2}. \end{aligned} \quad (18)$$

Each of these field values may then be related using a single first-order node basis finite-element local matrix, and the resulting expression can be manipulated and simplified by substituting (2) to leave

$$r = -\frac{\epsilon_{z1} B_1 \sin a_1 - \epsilon_{z2} B_2 \sin a_2}{\epsilon_{z1} B_1 \sin a_1 + \epsilon_{z2} B_2 \sin a_2} \quad (19)$$

where B_i and a_i are defined in (4) and (7) and the subscript i refers to either Material 1 or 2 in Fig. 3(a).

Similarly, projecting a plane wave onto the mesh fragment depicted in Fig. 3(b) results in the field values

$$\begin{aligned} H_1 &= (1 + r) & H_6 &= e^{-jb_1} (e^{-ja_1} + r e^{ja_1}) \\ H_7 &= (1 + r) e^{ja_2} e^{-jb_2} & H_8 &= (1 + r) e^{ja_2} e^{jb_2} \\ H_9 &= e^{jb_1} (e^{-ja_1} + r e^{ja_1}) & H_{10} &= H_5 e^{-2jb_1} \\ H_{11} &= H_4 e^{-2jb_2} & H_{12} &= H_3 e^{2jb_2} \\ H_{13} &= H_2 e^{2jb_1}. \end{aligned} \quad (20)$$

These field values can be related using five first-order edge basis finite-element local matrices to produce the system of

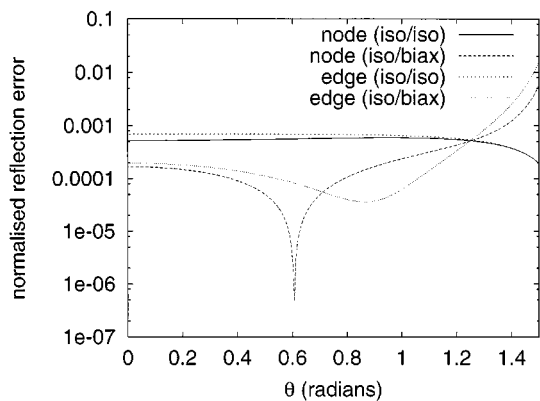


Fig. 4. The predicted reflection error for node and edge basis functions given by (19) and (22) for the interface between two isotropic media and also an interface between an isotropic and an anisotropic media. In each case, $c_{x1} = c_{y1} = 0.1$ and $c_{x2} = 0.2$ with c_{y2} being either 0.2 or 0.1 for isotropic or biaxial cases, respectively.

equations

$$\begin{bmatrix} 2C'_1 e^{jb} & 0 & 0 & 2D'_1 \cos(b) & B'_1 (e^{ja_1} + e^{jb}) \\ 0 & 2C'_2 e^{jb} & 2D'_2 \cos(b) & 0 & B'_2 (e^{ja_2} + e^{jb}) \\ 0 & 2D'_2 \cos(b) & 2C'_2 e^{-jb} & 0 & B'_2 (e^{ja_2} + e^{-jb}) \\ 2D'_1 \cos(b) & 0 & 0 & 2C'_1 e^{-jb} & B'_1 (e^{ja_1} + e^{-jb}) \\ B'_1 & B'_2 & B'_2 & B'_1 & (A'_1 + A'_2) \end{bmatrix} \begin{bmatrix} H_2 \\ H_3 \\ H_4 \\ H_5 \\ r \end{bmatrix} + \begin{bmatrix} B'_1 (e^{jb} + e^{-ja_1}) \\ B'_2 (e^{jb} + e^{ja_2}) \\ B'_2 (e^{-jb} + e^{ja_2}) \\ B'_1 (e^{-jb} + e^{-ja_1}) \\ (A'_1 + A'_2) \end{bmatrix} = 0 \quad (21)$$

the solution to which can be found, using (13), as

$$r = -\frac{Z_1 - Z_2}{Z_1 + Z_2} \quad (22)$$

where

$$Z_i = \frac{(D'_i)^2 \cos^2 b - 4(C'_i)^2}{B'_i{}^2 (D'_i - 2C'_i) \sin a_i} \quad (23)$$

and the terms a_i , b_i and B'_i , C'_i , D'_i are defined in (7) and (8) and (15)–(17). Again, the subscript i indicates either Material 1 or 2 in Fig. 3(b).

The above equations were used to model the error in the reflection coefficient of a plane wave incident on a dielectric interface, depicted in Fig. 3 as a function of incident angle. Numerical reflection was calculated where Material 1 was air and Material 2 was either an isotropic dielectric with $\epsilon_r = 2$ or an anisotropic dielectric with $\epsilon_y = 2$, $\epsilon_x = \epsilon_z = 1$. A plane wave with magnetic field polarized in the z -direction was chosen such that both x - and y -components of the anisotropic dielectric tensor would contribute to the plane wave propagation characteristics.

Fig. 4 presents the predicted numerical reflection error, being the difference between the reflection predicted by (19) and (22) for node and edge basis functions, respectively, and the exact reflection predicted using Maxwell's equations as a function of incident angle.

Interestingly, in the isotropic cases, the reflection errors of both node and edge basis functions are very similar. When Material 2 is made anisotropic, the reduction in the average dielectric

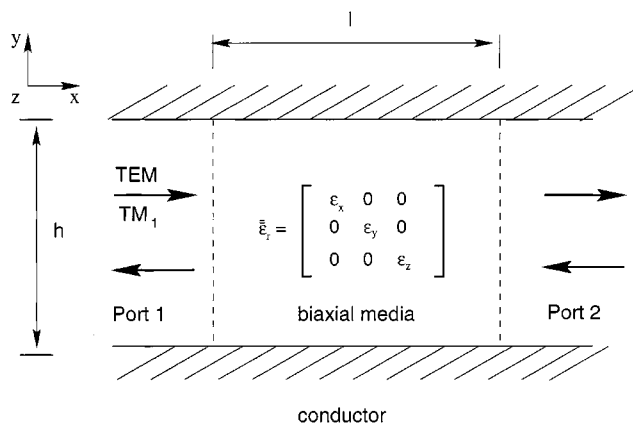


Fig. 5. The waveguide geometry used to examine the dispersion error.

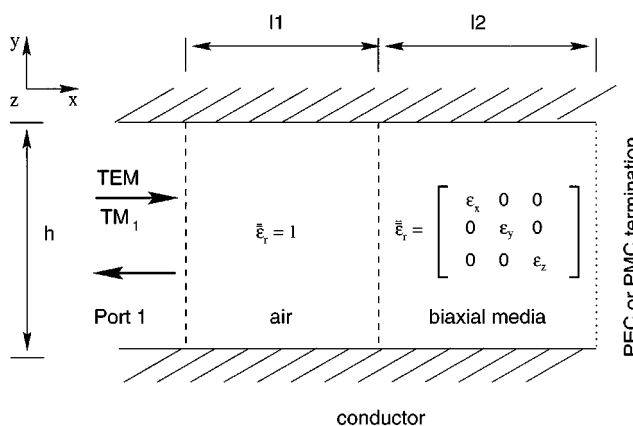


Fig. 6. The waveguide geometry used to examine the reflection error.

of the material has caused the normal incidence reflection error to reduce for both node and edge basis functions. At a specific angle, the numerical reflection of the nodal case involving biaxial material exactly equals the exact reflection causing a sharp null in the reflection error.

III. VERIFICATION

Having derived the closed-form expressions for numerical dispersion and numerical reflection for both node and edge basis functions of the first order, it is now necessary to verify that these expressions do indeed represent the numerical errors that will be exhibited by a practical finite-element simulation using these basis functions. The derivation of (19) and (22) were performed assuming that the mesh in question was composed of identical equilateral triangles configured in a hexagonally symmetric pattern. In most practical problems, this will not be the case. Most mesh generators—for example, [9]—will attempt to produce equilateral triangles of a given area but are constrained to fit the geometry of the problem. It is the purpose of this section to demonstrate that the biaxial dispersion and reflection simulated for a practical finite-element problem on a nonideal mesh is well approximated by the ideal derivations of the previous section.

Simple geometries, consisting of a parallel plate waveguide filled with dielectric material as shown in Figs. 5 and 6, were used to verify dispersion and reflection errors, respectively. The

mesh generator “Triangle1.3” [10] was used to discretize this geometry into triangles with a minimum interior angle of 28° .

A guided wave was coupled into the problem through Port 1, such that it propagated through the waveguide and, for the dispersion error simulation, was coupled out of the problem through Port 2 of Fig. 5. For the reflection error simulation, the wave was transmitted through an interface and then reflected from either a perfect electric conductor (PEC) or perfect magnetic conductor (PMC) termination and returned to Port 1. To examine the isotropic cases, a TEM wave was used to excite the waveguide, corresponding to a plane wave propagating along the x -direction. For the anisotropic case, the TM_1 mode of the waveguide was used since that mode would be affected by both x - and y -components of the material tensors. This first-order mode can be thought of as the superposition of two plane waves propagating at an angle θ to the x -axis, where

$$\theta = \sin^{-1} \left(\left(\frac{m\pi}{h} \right) \frac{1}{k_0 \sqrt{\mu_x \epsilon_x}} \right) \quad (24)$$

where

- m order of the mode;
- h width of the waveguide;
- k_0 $2\pi/\lambda$.

It is expected that an amount of numerical error equivalent to that of the dispersion and reflection may occur when coupling power into and out of the simulation through the ports. Thus it is necessary to de-embed the dispersion and reflection parameters from the model. To do this, multiple simulations with slight variations in the geometry are performed. The results of these simulations are combined to yield the desired parameters. The details of the de-embedding procedures used can be found in [11].

A. Verification of the Numerical Dispersion Error

Three parameters of a finite-element simulation contribute to the numerical errors, frequency, mesh edge length, and amplitude of the materials dielectric constant. The contributions from each of these parameters have been combined in c_x and c_y [(9) and (10)], respectively. To verify that (2) does indeed represent the dispersion error evident in a practical finite-element simulation, the geometry of Fig. 5 has been simulated with each of these parameters varied independently. The range of parameters used in the simulation is given in Table I.

Fig. 7(a) presents the de-embedded numerical dispersion error for the geometry of Fig. 5 when node basis functions are used. Results for the TEM wave propagating through isotropic material and the TM_1 mode propagating through biaxial media are labeled (iso) and (biax) respectively. Excellent agreement is observed between the predicted and simulated results for nodes with both isotropic and anisotropic media.

The above investigation was repeated using edge basis functions, and the results are presented in Fig. 7(b). Although good agreement is achieved for the biaxial case, there is a stark difference between the predicted and observed dispersion error for the isotropic simulation.

The predicted dispersion (solid line) is very low and exhibits a fourth-order dependence on c_x , as suggested by [2]. The disper-

TABLE I
VARIABLES USED IN THE INVESTIGATION OF NUMERICAL DISPERSION IN A PARALLEL-PLATE WAVEGUIDE LOADED WITH ISOTROPIC DIELECTRIC (iso) AND BIAXIAL DIELECTRIC (biax)

Variable	k_0	L (cm)	$\sqrt{\epsilon_x \mu_z}$	$\sqrt{\epsilon_y \mu_z}$	c_x
k_0 (iso)	1 - 3	0.045	1	1	0.045-0.135
L (iso)	1	0.03 - 0.15	1	1	0.03-0.1
ϵ (iso)	1	0.045	1 - 5.5	1 - 5.5	0.045-0.3
L (biax)	1	0.03 - 0.15	1	2	0.03-0.1

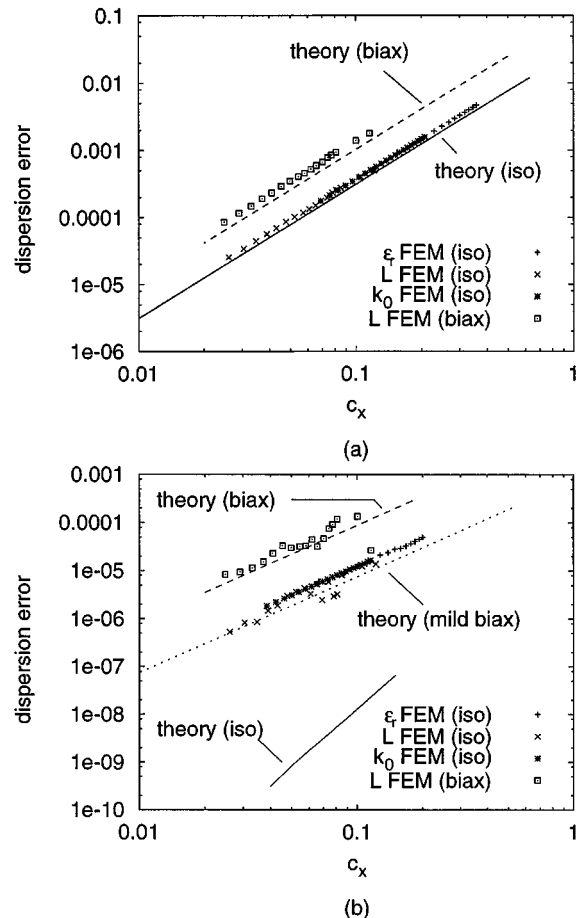


Fig. 7. Simulated and predicted dispersion error for (a) node and (b) edge basis functions using the geometry of Fig. 5. Isotropic case: +, × and * represent FEM solution with varying ϵ_r , L , and k_0 respectively, while the solid line represents the solution to (a) [(2)] or (b) [(13)] with $\theta = 0$. Biaxial case: □ represents the FEM solution for the TM_1 mode; dashed line represents solution of either (a) [(2)] or (b) [(13)] at an angle given by (24), with dotted line in (b) representing mild anisotropy.

sion evident in the practical FEM simulation is much higher, exhibiting a second-order dependence on c_x . This is to be expected for a mesh containing nonequilateral triangles as observed in [2].

Distortion of a triangular element could be approximated by an anisotropic contribution from mesh edge length to c_x and c_y . To examine this, a very small amount of anisotropy ($\epsilon_x = 1.0$, $\epsilon_y = 1.1$) was introduced to the material in (13), and the numerical dispersion was averaged over all mesh orientations, taking care to hold the orientation of the material static. The results of

TABLE II
VARIABLES USED IN THE INVESTIGATION OF NUMERICAL REFLECTION OF THE FUNDAMENTAL TE MODE FROM AN INTERFACE BETWEEN TWO ISOTROPIC DIELECTRIC MATERIALS WITHIN A PARALLEL PLATE WAVEGUIDE

Variable	$l_1 = l_2$ (cm)	k_0	L_{edge} (cm)	$\sqrt{\epsilon_{x1}\mu_{z1}}$	$\sqrt{\epsilon_{x2}\mu_{z2}}$	$\sqrt{\epsilon_{y2}\mu_{z2}}$	c_{x1}
k_0 (iso)	0.25	1 – 3	0.045	1	2	2	0.045-0.135
L (iso)	0.75	1	0.03 – 0.1	1	2	2	0.03-0.1
ϵ (iso)	0.25	1	0.045	1 - 4	2-8	2-8	0.045-0.18
L (biax)	0.75	1	0.03 – 0.1	1	1	2	0.03-0.1

this procedure are presented in Fig. 7(b) as a dotted line. This is evidently a much better fit to the numerical dispersion observed in practice. Further investigation may reveal a rule-of-thumb method for producing an effective anisotropy to insert in the equation (refedge-dispersion) that could be derived from the statistics of the mesh imperfections.

B. Numerical Reflection Error

The approach used in the previous section to verify the closed-form expressions for dispersion error for the edge and node basis functions was applied to the assessment of (19) and (22) in approximating the numerical reflection error for a practical finite-element simulation. The geometry of Fig. 6 was simulated using an FEM with the parameters summarized in Table II.

Fig. 8(a) presents the de-embedded numerical reflection error for the geometry of Fig. 6 when node basis functions are used. Results for the TEM wave incident on an interface between two isotropic materials and the TM_1 mode incident on the interface between an isotropic material and an anisotropic material are labeled (iso) and (biax), respectively. Good agreement is achieved for the isotropic case with the reflection error from the practical finite-element simulation being slightly higher than that predicted by (19). The abrupt behavior observed with the frequency set to give $c_x \approx 0.18$ is due to a resonance of the structure being excited. This causes the FEM matrix to become poorly conditioned and introduces further numerical inaccuracies.

Reasonable agreement is also achieved for the biaxial case in Fig. 8(a); however, it is interesting to note that the observed reflection error from the FEM exhibits a significant amount of noise and is in general below that predicted by (19). An explanation may be found by considering that the effective angle of incidence (24) is close to the sharp feature of zero reflection error observed in Fig. 4. Small variation in the different meshes used to model this interface may have adjusted the location of this feature and hence may have caused the noisy but lower than expected reflection error observed.

The verification of the numerical reflection error relations was repeated using edge basis functions with results presented in Fig. 8(b). Again, the reflection error is higher than expected for both isotropic/isotropic and isotropic/biaxial interfaces. This could be attributed to the imperfection of the practical mesh used in the FEM simulation causing larger than predicted numerical dispersion in the isotropic media.

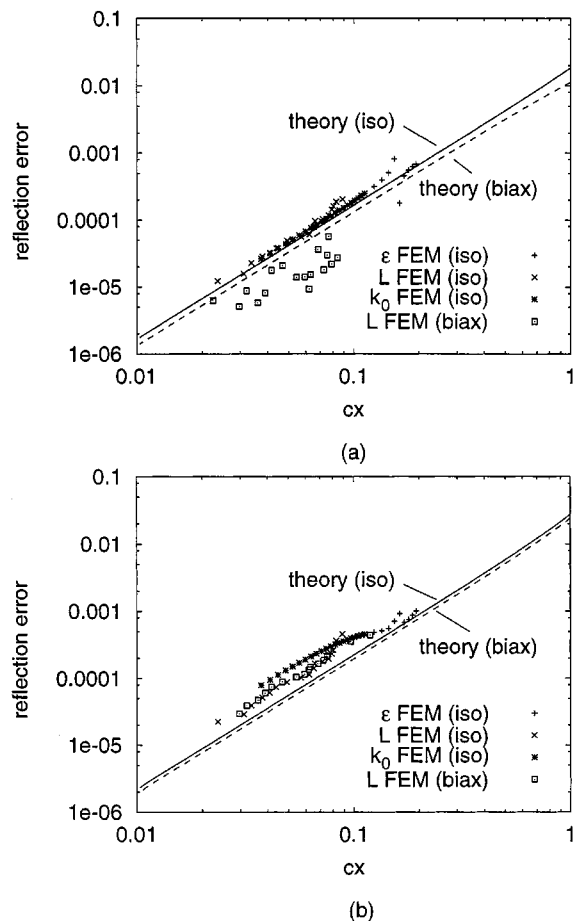


Fig. 8. Simulated and predicted reflection error for (a) node and (b) edge basis functions using the geometry of Fig. 6. Isotropic case: +, x, and * represent FEM solution with varying ϵ_r , L , and k_0 , respectively, while solid line represents the solution to (a) [(19)] or (b) [(22)] with $\theta = 0$. Biaxial case: \square represents the FEM solution for the TM_1 mode, and dashed line represents solution of either (a) [(19)] or (b) [(22)] at an angle given by (24).

IV. CONCLUSION

Closed-form expressions for the numerical dispersion and reflection errors for edge and node basis functions have been developed, assuming a perfect hexagonal mesh for biaxial materials. The applicability of these models to practical simulations has been investigated by de-embedding the numerical dispersion and reflection errors from FEM simulation results of parallel plate waveguide geometries. It is evident that the relations for numerical dispersion (2) and (13) and numerical reflection (19) and (22) for node and edge basis functions, respectively,

provide good models for the imperfect meshes of practical simulations, although imperfections in the mesh must be accounted for when using (13) with isotropic media.

Having verified these expressions as valid estimations of the numerical errors that can be expected in practical simulations, it may now be possible to use these expressions to guide the choice of mesh parameters for problems involving biaxial media. As mentioned previously, a particularly important application for these closed-form expressions will be in the investigation of the nature of reflection errors that occur at theoretically reflectionless PML boundaries. The use of the closed-form expressions derived in this paper in the analysis and optimization of PML boundaries in the finite-element method is currently under investigation.

REFERENCES

- [1] G. S. Warren and W. R. Scott, "An investigation of numerical dispersion in the vector finite element method using quadrilateral elements," *IEEE Trans. Antennas Propagat.*, vol. 42, pp. 1502–1508, Nov. 1994.
 - [2] —, "Numerical dispersion in the finite element method using triangular edge elements," *Microwave Opt. Technol. Lett.*, vol. 9, pp. 315–319, Aug. 1995.
 - [3] —, "Numerical dispersion of higher order nodal elements in the finite-element method," *IEEE Trans. Antennas Propagat.*, vol. 44, pp. 317–320, Mar. 1996.
 - [4] J. P. Bérenger, "A perfectly matched layer for the absorption of electromagnetic waves," *J. Comput. Phys.*, vol. 114, no. 2, pp. 185–200, Oct. 1994.
 - [5] A. C. Polycarpou, M. R. Lyons, and C. A. Balanis, "A two dimensional finite element formulation of the perfectly matched layer," *IEEE Microwave Guided Wave Lett.*, vol. 6, pp. 338–340, Sept. 1996.
 - [6] J. Fang and Z. Wu, "Closed-form expression of numerical reflection coefficient at PML interfaces and optimization of PML properties," *IEEE Microwave Guided Wave Lett.*, vol. 6, pp. 332–334, Sept. 1996.
 - [7] A. Mitchell, J. T. Aberle, D. M. Kokotoff, and M. W. Austin, "An anisotropic pml for use with biaxial materials," *IEEE Trans. Microwave Theory Tech.*, vol. 47, pp. 374–377, Mar. 1998.
 - [8] J. Jin, *The Finite Element Method in Electromagnetics*. New York: Wiley, 1993.
 - [9] J. R. Shewchuk, "Triangle: Engineering a 2d quality mesh generator and Delaunay triangulator," in *Proc. 1st Workshop Applied Computational Geometry ACM*, May 1996.
 - [10] —, "Triangle 1.3: A two-dimensional quality mesh generator and Delaunay triangulator," School Comput. Sci., Carnegie-Mellon Univ., Pittsburgh, PA, Software, 1996.
 - [11] A. D. Mitchell, "Efficient PML boundaries for anisotropic waveguide simulations using the finite element method," Ph.D. dissertation, Royal Melbourne Inst. of Technol., Australia, 1999.
- Arnan Mitchell**, photograph and biography not available at the time of publication.
- David M. Kokotoff** (S'84–M'84), photograph and biography not available at the time of publication.
- Michael W. Austin** (M'83), photograph and biography not available at the time of publication.